

# Origin of the $T_c$ depression and the role of charge transfer and dimensionality in ultrathin $\text{YBa}_2\text{Cu}_3\text{O}_{7-\delta}$

Marta Z. Cieplak

*Department of Physics and Astronomy, Rutgers University, Piscataway, New Jersey 08855  
and Institute of Physics, Polish Academy of Sciences, Warsaw, Poland*

S. Guha and S. Vadlamannati

*Department of Physics and Astronomy, Rutgers University, Piscataway, New Jersey 08855*

T. Giebultowicz

*Department of Physics, George Mason University, Fairfax, Virginia 22030*

P. Lindenfeld

*Department of Physics and Astronomy, Rutgers University, Piscataway, New Jersey 08855*

(Received 16 March 1994; revised manuscript received 18 July 1994)

We describe measurements on trilayers and multilayers of  $\text{YBa}_2\text{Cu}_3\text{O}_{7-\delta}$  (YBCO) with intervening layers of  $\text{Y}_{1-x}\text{Pr}_x\text{Ba}_2\text{Cu}_3\text{O}_{7-\delta}$ , with thicknesses  $d$  of YBCO down to that of a single unit cell. The zero-resistance transition temperature,  $T_{co}$ , decreases as  $d$  decreases, and increases as  $x$  decreases, and we show that a single unit-cell layer is still superconducting. We describe a transition from a “bulk regime” in the interior of the YBCO to a “surface regime” near the interfaces, and show that the  $T_{co}$  depression is correlated with a depressed conductance in the region adjacent to the interfaces. The results indicate that the changes are related to the presence of the interfaces, primarily to charge transfer between the layers, with only minor indications of a change in the intrinsic properties of the YBCO from the bulk down to the thickness of a single unit cell. The values of  $T_{co}$  in multilayers are consistent with those on trilayers, and so rule out any contributions from very long-range interactions, but they indicate the presence of interactions with length scales of several hundred angstroms across the barrier layers.

## I. INTRODUCTION

From the earliest days after the discovery of cuprate superconductivity it has been apparent that the dimensionality of the conducting paths plays a central role in the realization of the superconducting properties. One of the most direct ways to investigate this question is to make ultrathin films, and the first descriptions of experiments on films down to thicknesses of one or two unit cells were reported in 1990.<sup>1-3</sup> It is typical of the difficulty of making well-characterized specimens and reliable measurements that the experiments disagreed on the question whether films of  $\text{YBa}_2\text{Cu}_3\text{O}_{7-\delta}$  (YBCO) with a thickness equal to that of a single unit cell were superconducting. In spite of mounting evidence this question is still somewhat controversial.<sup>4-7</sup> In this paper we not only present evidence that such films are indeed superconducting, but also that the observed reduction in their transition temperature, measured when they form part of artificial multilayer structures, is predominantly of extrinsic origin, i.e., that it is not primarily a property of the ultrathin films themselves.

This conclusion is in contrast to the widespread assumption that the reduction of the transition temperature indicates the necessity of transverse coupling, i.e., of some amount of three-dimensionality for the full de-

velopment of the superconducting properties in YBCO. The conclusion also removes the apparent discrepancy with the results on ultrathin films of  $\text{Bi}_2\text{Sr}_2\text{CaCu}_2\text{O}_8$  which do not exhibit a corresponding decrease in transition temperature.<sup>8</sup>

The results on multilayers could conceivably be influenced by long-range magnetic interactions between the superconducting layers. In order to avoid this complication a large part of our work has been on trilayers containing only a single superconducting layer. By making measurements on structures in which the thickness of the superconducting layer is varied in steps of a few angstroms we are able to follow the evolution of the superconducting properties and to demonstrate the superconductivity of single-unit-cell layers.

A principal result is that the variation in transition temperature with thickness is correlated with corresponding changes in the normal-state conductance per square. It is this feature that shows that the interfaces to the adjacent material play the predominant role in changing the transition temperature. The results indicate a distinction between a “surface regime” strongly influenced by the different neighboring layers, and a “bulk regime” in thicker films in which the interfaces play only a minor role.

In Refs. 1-3 the superconducting layers were sep-

arated by "barrier layers" of nonsuperconducting  $\text{PrBa}_2\text{Cu}_3\text{O}_{7-\delta}$  (PrBCO). We have also made measurements with barrier layers of  $\text{Y}_{1-x}\text{Pr}_x\text{Ba}_2\text{Cu}_3\text{O}_{7-\delta}$  ([Y-Pr]BCO) that demonstrate that the properties of the YBCO layer are strongly influenced by the nature of the adjacent material.

The outline of the paper is as follows. In Sec. II we describe the specimen preparation. In Sec. III we discuss the characterization, structural analysis, and the growth mechanism. In Sec. IV we present the data on trilayers and in Sec. V those on multilayers.<sup>9</sup> Finally Sec. VI contains some further discussion, including comments on remaining open questions.

## II. SPECIMEN PREPARATION

The specimens were prepared by pulsed laser deposition from ceramic targets, using a 248-nm pulsed excimer laser with an energy of about 0.2 J per pulse, and a repetition rate of 2.5 pulses per sec. The targets were made from the powdered oxide constituents by the standard solid state reaction method, at 940 °C in flowing oxygen for 60 h.

The films were deposited on (100)  $\text{SrTiO}_3$  substrates held at 760 °C in an atmosphere of 100-mTorr oxygen. The deposition rate was about 0.4 Å per pulse. The specimens were annealed *in situ* at 400 °C and 600 mTorr oxygen for 30 min.

To calibrate the film thickness deposited per pulse several films with different thicknesses were measured with a profilometer. The uncertainty of this measurement is about 10%. Several films were also measured by Rutherford backscattering (RBS).

The laser power was monitored during deposition and manually controlled. Unavoidable fluctuations in the laser power give rise to some additional uncertainty in the thickness measurement, and contribute to the observed scatter of the measured points.

## III. SPECIMEN CHARACTERIZATION AND STRUCTURAL ANALYSIS

### A. Single films

As a first step we prepared films of  $\text{Y}_{1-x}\text{Pr}_x\text{Ba}_2\text{Cu}_3\text{O}_{7-\delta}$ , with values of  $x$  from zero to one, with thicknesses between 400 Å and 6000 Å. The specimens were characterized by x-ray diffraction, ac-susceptibility, and resistivity measurements. Particular attention was paid to compositions in the vicinity of the metal-insulator (MI) transition, i.e., near  $x = 0.55$ .

X-ray diffraction showed the samples to be *c*-axis oriented. No peaks other than (001) are observed, indicating the absence of misaligned grains.

Rutherford backscattering and channeling were measured with a 1.7-MeV Tandatron. Figure 1 shows the results for a sample with  $x = 0.50$ . The continuous line is a simulation that is seen to fit the experimental results very well. The channelling yield is about 3%, similar to that observed for *c*-axis aligned YBCO films in previous determinations.<sup>10</sup>

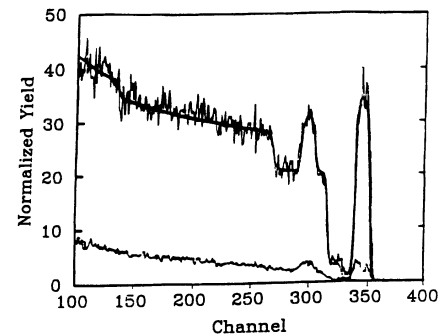


FIG. 1. Rutherford backscattering spectrum for a (Y-Pr)BCO film with  $x = 0.50$ . The upper curve is the random yield, and the lower curve is the channeling yield.

Figure 2 shows the temperature dependence of the *ab*-plane resistivity for films with various values of  $x$ . For pure YBCO ( $x = 0$ ) the resistivities at 300 K and 100 K are 270  $\mu\Omega\text{cm}$  and 80  $\mu\Omega\text{cm}$ , respectively, with an extrapolated zero-resistivity intercept close to  $T = 0$  and a transition width of about 0.5 K. The MI transition is close to  $x = 0.55$ , as previously observed.<sup>11,12</sup> The variation of  $T_c$  with  $x$  is shown in Fig. 3, where the vertical lines indicate the 10 – 90 % widths. The ac-susceptibility measurements show that the flux is expelled primarily at the temperature where the resistance goes to zero, even though the resistance begins to decrease at the onset temperature  $T_c^{(\text{on})}$ , which can be considerably higher.

For films close to the MI transition there is a substantial dependence of the transition temperature on film thickness. With  $x = 0.50$ , for a 2000-Å-thick specimen,  $T_{co} = 25$  K, while for a 600 Å film of the same composition no sign of superconductivity is observed down to 4.2 K. As the thickness decreases, the temperature dependence also develops the upturn at low  $T$  that is characteristic of increased carrier localization.

An even stronger thickness dependence, persisting to several thousand Å has previously been observed in  $\text{La}_{1.85}\text{Sr}_{0.15}\text{CuO}_4$  films and ascribed to strain resulting from lattice mismatch to the substrate.<sup>13</sup> In view of the much smaller mismatch for (Y-Pr)BCO we regard this explanation as unlikely to explain our results, and we are

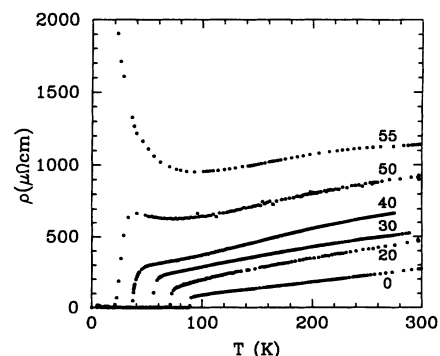


FIG. 2. The resistivity parallel to the substrate for a series of films with various values of  $x$ .

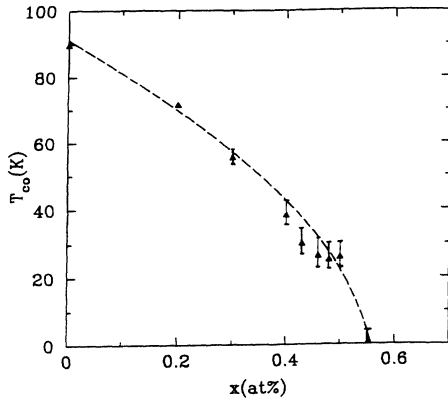


FIG. 3. The transition temperature of a series of films as a function of  $x$ .

therefore continuing experiments to gain a better understanding of the thickness dependence.

### B. Structural disorder in ultrathin films and multilayers

In contrast to thick films, superconductivity in ultrathin films and multilayers is strongly dependent on the type and amount of structural disorder at the interface between the superconducting layers and the intervening “barrier layers.” Interdiffusion of the rare-earth elements and atomic-scale steps at the boundary contribute to the growth of a mixed layer of (Y-Pr)BCO that affects superconductivity adversely, particularly in films whose thickness is close to that of a single unit cell. Estimates of this type of discrete disorder vary between different laboratories, from “negligible” to about 30% of rare-earth mixing in the layer adjacent to the interface.<sup>7,14–17</sup> The large variation indicates that the degree of disorder depends on the particular growth method. Electron microscopy studies show that there are also large-scale lateral steps that occur as a result of growth nucleation in the form of islands in the  $ab$  plane. The islands subsequently expand in the lateral direction to create growth terraces that eventually coalesce. Various lattice defects, such as dislocations and stacking faults, may occur and contribute to the large-scale lattice disorder and to thickness fluctuations in the multilayer structures.<sup>14,15</sup>

To assess the various types of disorder in our ultrathin films, measurements were made of low-angle x-ray reflectivity and high-angle x-ray diffraction on the YBCO/PrBCO superlattices. Low-angle reflectivity is particularly sensitive to the interface morphology.<sup>18</sup> Atomic-scale disorder, as well as steps at the boundary of growth terraces, modify the x-ray scattering density profile throughout the interface. In addition any fluctuation in the layer thickness will broaden the superlattice peaks. By fitting the reflection spectrum with a simulation based on a structural model of the multilayer one can estimate the “roughness layer” resulting from interdiffusion and steps, and evaluate the magnitude of the layer-thickness fluctuation. A complementary picture of the structural disorder may be obtained from the model-

ing of the high-angle diffraction spectrum which provides, in addition, information about the lattice parameters and the strain in the multilayer.<sup>17,19</sup>

Low-angle x-ray reflectivity measurements were made at the National Institute for Science and Technology. Figure 4 shows the results for a superlattice of alternating layers of 3 unit cells of YBCO and 10 unit cells of PrBCO, together with a line resulting from a fit to a numerical model.<sup>18</sup>

The model includes an “interface roughness” parameter which describes interdiffusion and relatively small terraces or islands. Such defects lead to a weakening of the intensity of the superlattice peaks. The results indicate a roughness layer up to  $\pm 10$  Å, i.e., a little less than a single-cell thickness. There is also some line broadening, corresponding to thickness fluctuations of about  $\pm 2$  Å, resulting from a lack of uniformity of the thickness of the Y-Pr bilayers.

The high-angle diffraction spectra were measured at the University of California in San Diego by Hasen and Schuller. They are preliminary results of a comprehensive study that we expect to provide further detailed structural information. The results shown in Fig. 5 are for a multilayer with seven unit-cell layers of PrBCO separating the YBCO layers whose thickness is 16 Å (specimen *B*). A similar study was also made for a second specimen (specimen *A*) with a YBCO thickness of 12 Å.

The structural model that was used to provide a fit to the data was described in Refs. 19 and 17. The interdiffusion into the first adjacent unit cell is about 11% for both specimens, but a large difference between the two samples is found in the thickness fluctuation. For sample *A* it is 8 Å and for sample *B* it is 4 Å. For sample *A* the indicated filling of the area by a single-unit-cell thick layer is 55%, with the remaining area divided about equally between zero coverage and a two-unit-cell layer. For sample *B* the covered area is about 95%, with a little more than a third of it covered by a two-unit-cell layer.

Clearly the coverage for the 12 Å specimen (*A*) is far from uniform, with islands connected by paths barely past the percolation threshold. A considerable increase in

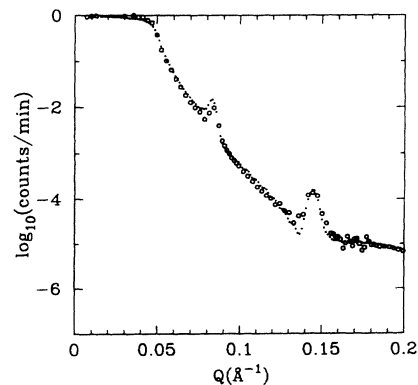


FIG. 4. Low-angle x-ray diffraction spectrum for a multilayer specimen of YBCO/PrBCO, with 36 Å of YBCO, 117 Å of PrBCO, repeated 20 times. The dotted line is a fit to the numerical model.

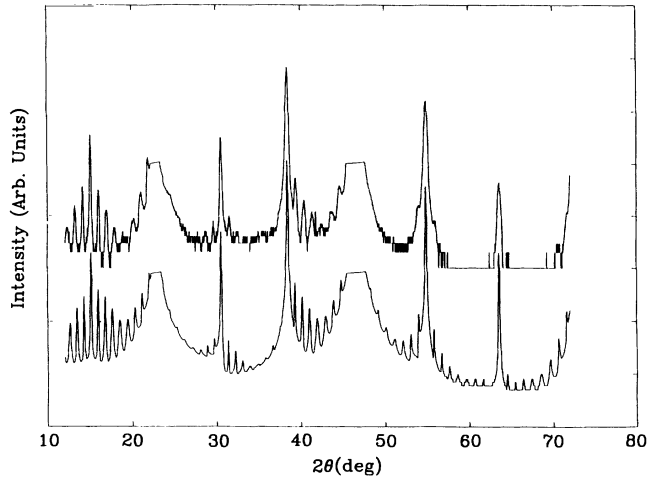


FIG. 5. The upper curve is the x-ray spectrum of a multilayer specimen of 16 Å YBCO and 82 Å PrBCO, repeated 19 times. The lower curve shows the corresponding simulation.

uniformity, with almost complete coverage, is, however, achieved with the deposition of four additional Å in the YBCO layer.

Even though the results of the structural studies are quite preliminary, they tend to indicate that our multilayer specimens are similar to the best that have been described previously, with disorder and a small amount of interdiffusion confined to the unit-cell layer adjacent to the interface. With a nominal thickness just equal to one unit-cell layer, the coverage is quite incomplete, but becomes almost complete and considerably more uniform with an increase in thickness of just a few more Å.

#### IV. TRILAYERS

##### A. YBCO/PrBCO

The trilayers were deposited on (100)  $\text{SrTiO}_3$ , with a 400 Å bottom layer of PrBCO, followed by a thickness  $d$  of YBCO, and capped by 200 Å of PrBCO. For some of the specimens the transition temperature was first determined by a contactless ac-susceptibility measurement. A four-terminal pattern was then scribed on the specimen with a diamond scribe. Initially photolithography was used, but later abandoned because it seemed desirable to avoid processing as much as possible. Four indium pads were cold pressed on the sample.

The resistivity was measured with the help of a computer-controlled data acquisition system. The specimen was in a sample holder that was manually lowered in the vapor of a liquid-helium storage vessel while  $R(T)$  was measured from room temperature to 4.2 K. The current density was of the order of 1–10  $\text{A}/\text{cm}^2$ , with a linear response in this region. Some specimens had curves of  $R(T)$  with discontinuities, possibly because of cracks or other damage, and were not used. A few had long tails which we interpret as resulting from inhomogeneities, and were also rejected.

Figure 6(a) shows the total resistance per square of

some of the trilayer specimens as a function of temperature. The specimen with  $d = 11$  Å exhibits the quasireentrant form typical for island formation below the percolation threshold and was therefore not further analyzed. In the specimen with  $d = 9$  Å the conduction path seems to be somewhat better connected. This is not unreasonable since close to the percolation threshold the nature of the conduction path is subject to considerable randomness. As the YBCO thickness increases, superconducting transitions are observed with increasing transition temperatures. Also shown on the figure is a curve with only the 600 Å of PrBCO, deposited and patterned as for the trilayers.

For the curves of Fig. 6(b) the conductance of the PrBCO was subtracted, assuming it to be the same as that measured separately and shown in Fig. 6(a). This may not be quite correct, since the layer of PrBCO close to the interface is likely to be affected by the vicinity of the YBCO, as discussed in Sec. IVE. As  $d$  increases, the curves are seen to be linear in the normal state, with gradually decreasing intercept.

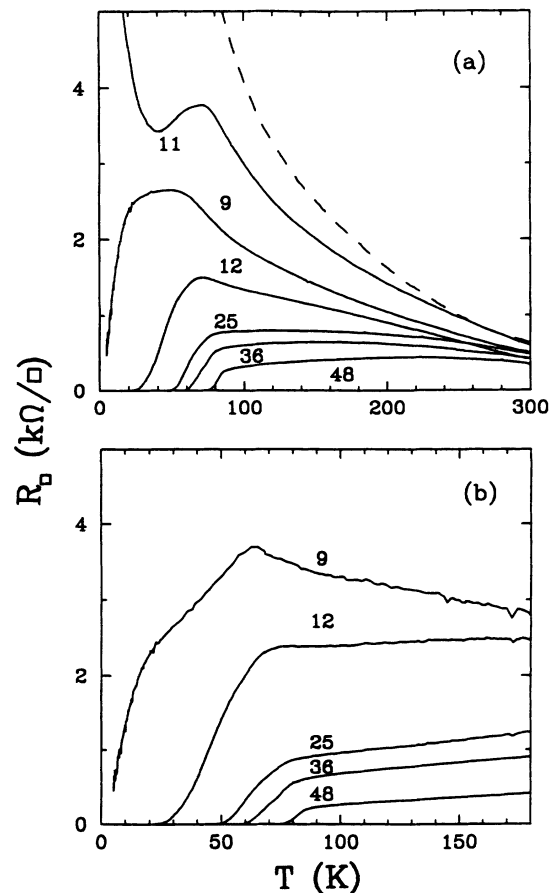


FIG. 6. (a) Resistivity per square as a function of temperature for a series of YBCO/PrBCO trilayer specimens with varying values of the YBCO thickness  $d$ . The dashed line is for pure PrBCO. (b) Resistivity per square as a function of temperature for a series of YBCO/PrBCO trilayer specimens after subtracting the contribution of the PrBCO layers to the conductance.

The temperature  $T_{co}$  was determined from semilog plots of  $R$  as a function of  $T$ , as the temperature where  $R$  has fallen to about  $0.1 \Omega$ , which is in all cases less than 1/10% of the extrapolated normal-state value,  $R_N$ .

Figure 7 shows  $T_{co}$  as a function of  $d$ . The dashed line is a guide to the eye, drawn to emphasize the evolution of the YBCO, one unit-cell thickness at a time. In order to test the existence and validity of the steps we have calculated the rms deviation both from a step curve and a least-squares fitted smooth curve, from  $d = 11 \text{ \AA}$  to  $d = 48 \text{ \AA}$ . The step curve has horizontal plateaus at 19.8, 38.8, and 67.8 K, joined by straight lines. The rms deviation of the measured points from this curve is 2.4 K. Their rms deviation from the smooth curve is 5.7 K. Somewhat similar steps have been noted by Triscone *et al.*<sup>20</sup>

The good fit to the line with the steps does not necessarily imply that the YBCO is deposited one unit-cell layer at a time, one after the other. It is, rather, consistent with the following sequence. At first the YBCO is deposited as unconnected islands, while the conductance remains zero. The conductance becomes finite when the percolation threshold is reached, i.e., when the first continuous conduction path is established, presumably when the coverage rises beyond about 50%. As more YBCO is deposited some of it may begin to form a second layer before the first layer is complete. The second layer will not, however, contribute significantly to the conductance and hence to the observed transition temperature until the percolation threshold is surpassed there also. Separate islands in the second layer will have little effect because of the large anisotropy, i.e., because of the high resistivity in the  $c$  direction. This description is supported by the discussions of the pattern of film growth in Refs. 14, 15, and 21.

The stepwise development is also evident on Fig. 8, which shows the conductance per square of the YBCO (after the subtraction of the PrBCO) as a function of  $d$ . As on the previous figure, the steps become less distinct after the first two or three, as a regime is reached that is characterized by a bulk resistivity  $\sigma$ , with a linear relationship between  $R_{\square}$  and  $d$ .

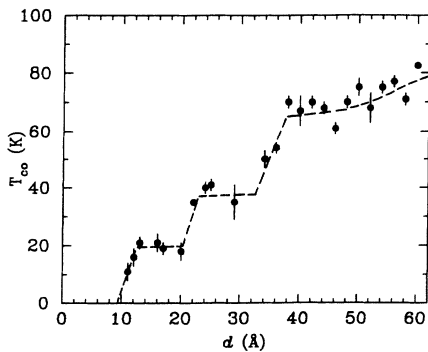


FIG. 7.  $T_{co}$  for a series of YBCO/PrBCO trilayer specimens with different values of the YBCO thickness  $d$ . The dashed line is discussed in the text.

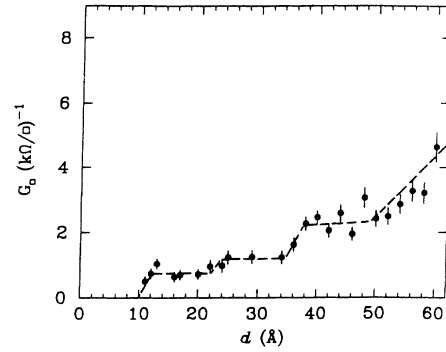


FIG. 8. The resistivity per square,  $G_{\square}$ , for the same series of specimens as for Fig. 7. The right-hand portion of the dashed line has a slope corresponding to a bulk resistivity of  $60 \mu\Omega \text{ cm}$ .

## B. YBCO/(Y-Pr)BCO

We have measured two further series of specimens, with barrier layers of  $\text{Y}_{1-x}\text{Pr}_x\text{Ba}_2\text{Cu}_3\text{O}_{7-\delta}$  with values of  $x$  of 0.50 and 0.55. For  $x=0.50$  the barrier layer is metallic. The value of 0.55 was chosen because it is close to the value at which the metal-insulator transition takes place, but we have not made the necessary measurements to determine on which side of the transition the barrier layers are in our specimens.

For these two series the subtraction of the barrier-layer conductance is subject to considerably more uncertainty than for the series described previously (with  $x = 1.0$ ), because the barrier-layer conductance represents a much greater fraction of the total conductance of the specimens. We have also measured fewer specimens. Nevertheless certain trends are evident on Figs. 9 and 10,

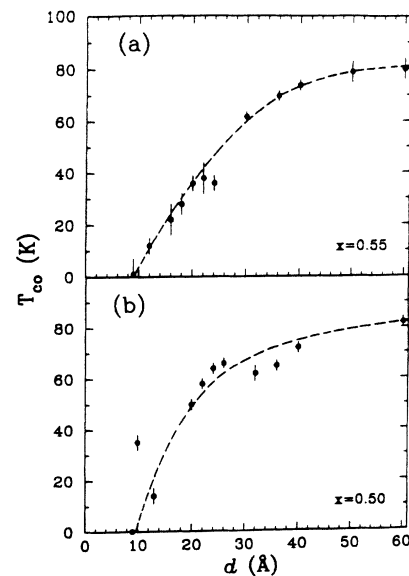


FIG. 9.  $T_{co}$  as a function of  $d$  for the trilayer series with (a)  $x = 0.50$  and (b)  $x = 0.55$ .

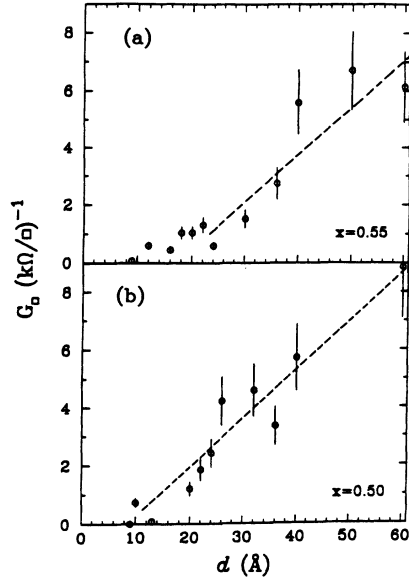


FIG. 10.  $G_{\square}$  as a function of  $d$  for the trilayer series with (a)  $x = 0.50$  and (b)  $x = 0.55$ . The right-hand portions of the dashed lines begin at a point  $(d_s, R_s)$ , and have slopes corresponding to a bulk resistivity of  $60 \mu\Omega \text{ cm}$ .

which show  $T_{co}$  and  $G_{\square}$  as a function of  $d$  for  $x = 0.50$  and  $x = 0.55$ .

The steps which we have discussed for the series with  $x=1.0$  are absent or, at least, less clear. This may be in part because of the smaller number of specimens, but probably also because the interfaces with the barrier layers do not represent as sharp a discontinuity between the two materials. The fact that in the barrier layers about half of the praeosdymium is replaced by yttrium mimics to some extent the result that would occur in the previous series (with  $x = 1.0$ ) from interdiffusion. Conversely, the absence of distinct steps here tends to confirm that interdiffusion does not play a large role in the earlier series.

The figures also show that for similar values of  $d$  the transition temperature and conductance tend to be higher. These features will be discussed in Sec. IV E.

### C. The relationship between the transition temperature and the conductance

The similarity in the stepwise progression of  $T_{co}$  with  $d$  and of  $G_{\square}$  with  $d$  suggests a comparison of  $T_{co}$  with  $G_{\square}$ . Figure 11, which shows the relation between these two quantities, reveals several striking features. The most interesting is that up to a conductance per square of about  $1.5 (\text{K}\Omega)^{-1}$  the two quantities are linearly related, within the uncertainties of the measurement, independently of the nature of the barrier layer. For larger values of  $G_{\square}$  there is a sharp bend or “knee,” beyond which the transition temperature saturates and increases slowly toward its ultimate limiting bulk value.

Regardless of the particular nature of the relationship between  $T_{co}$  and  $G_{\square}$ , regardless also of further theoretical analysis or speculation, the fact that the two quantities

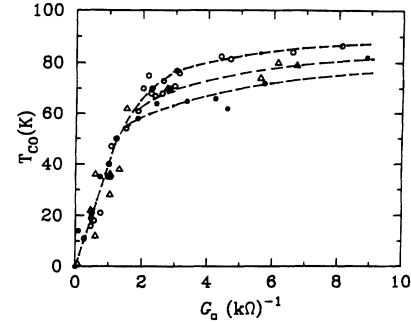


FIG. 11.  $T_{co}$  as a function of  $G_{\square}$  for the three series of trilayer specimens. The open circles are for  $x = 1.0$ , the triangles for  $x = 0.55$ , and the filled circles for  $x = 0.50$ .

are closely related implies that an understanding of the changes in the transition temperature is to be found in the parameters that determine the normal-state conduction, i.e., in the density of charge carriers and in their scattering processes.

To the extent that  $T_{co}$  depends entirely on  $G_{\square}$  it cannot depend on any features limited to the superconducting state, such as the superconducting proximity effect, which has no influence on  $G_{\square}$ . Of course this statement is limited by the uncertainties of our measurement. We do not wish to imply that there is no proximity effect, only that our results suggest that it does not play a major role in the decrease of the transition temperature with thickness.

We may go one step further. The parameters that determine  $G_{\square}$  are seen to be extrinsic, i.e., they depend on defects or on surface and interface properties characteristic of a particular specimen, but not on the fundamental, “intrinsic” nature of the YBCO itself. Again within the limitations of the measurement, and primarily in the region of the apparently unique linear relationship between  $T_{co}$  and  $G_{\square}$ , it seems that the decrease of the transition temperature with thickness is therefore not primarily an inherent, intrinsic property of the YBCO.

### D. The shape of the transition curve: Kosterlitz-Thouless transition and fluctuations

In a homogeneous bulk superconductor there is a single transition temperature and the sharpness of the transition is limited only by thermodynamic fluctuations. In a two-dimensional specimen the resistance does not, however, go to zero until a lower temperature  $T_{KT}$ , the Kosterlitz-Thouless (KT) transition temperature, where the spontaneously generated current vortices coalesce to form bound pairs. In contrast to the case of isotropic three-dimensional specimens the layered structure of high- $T_c$  materials gives rise to a KT transition also in bulk specimens or in relatively thick films, typically within about 1 K of the mean-field transition temperature.<sup>22</sup> In ultrathin films of YBCO the difference between  $T_{KT}$  and the mean-field transition temperature  $T_{mf}$  can be larger by more than an order of magnitude, as was first shown by Vadlamannati *et al.*<sup>23</sup> in multilayer structures of YBCO/PrBCO for YBCO thicknesses

of two and four unit-cell layers, and later by Matsuda *et al.*<sup>5</sup> for similar specimens with the thickness of a single unit-cell layer.

The existence of a KT transition gives rise to a variation of the resistance that follows the relation

$$\frac{R}{R_N} = A \exp -2\sqrt{\frac{b\tau_{mf}}{\tau}}, \quad (1)$$

where  $\tau = (T - T_{KT})/T_{KT}$ ,  $\tau_{mf} = (T_{mf} - T_{KT})/T_{KT}$ , and  $b$  is a constant. The most specific signature is, however, the nature of the  $I$ - $V$  curves, which follow the exponential form  $V = cI^m$ , where  $c$  is a constant, with a characteristic discontinuity in the exponent  $m$  from 3 to 1 at  $T_{KT}$ . Although the discontinuity is typically quite broad in the actual observations, the experiments described in Refs. 5 and 23 leave little doubt about the existence of a KT transition and the essential correctness of the theoretical description.

In the present experiments we have therefore not felt it necessary to prove the existence of a KT transition by making the necessary careful study of  $I$ - $V$  curves, but have been content to show that the resistance follows the form of Eq. (1), as shown for a specimen with  $d = 12$  Å in the inset to Fig. 12.

Surprisingly, it was much more difficult to fit the upper portion of the resistance transition, which is rounded by the effect of superconducting fluctuations, and for which a theoretical description has long been known and accepted.<sup>24</sup>

Our attempts to fit the upper part of the transition curve to the fluctuation expression with a single value of  $T_{mf}$  were not very successful. Much better results were achieved with a model in which the sample is assumed to consist of a chain of regions, each with its own mean-field transition temperature, with a Gaussian distribution (with standard deviation  $\sigma$ ) about an average mean-field transition temperature  $T_{mf}$ . The spread  $\sigma/T_{mf}$  is quite large for  $N = 1$  (25%) but reduces to less than 1% for  $N > 3$ . This variation is consistent with our realiza-

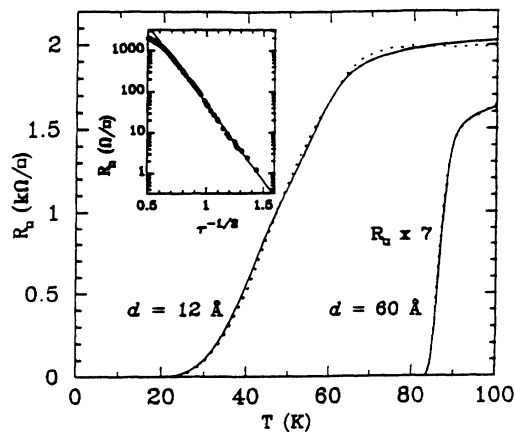


FIG. 12.  $R_{\square}(T)$  in the transition region for the YBCO part of two trilayer film specimens. The dotted lines are the data, and the continuous lines represent the fit described in the text. The inset shows a fit to Eq. (1).

tion that a single-unit-cell layer is quite disordered, as discussed in Sec. III D.

The mean-field transition temperature  $T_{mf}$  appears as a parameter both in the KT part of the curve just above  $T_{KT}$ , and in the fluctuation-dominated upper part. The fact that we obtained good fits for the whole transition curve with a single value of  $T_{mf}$ , as shown for two representative specimens on Fig. 12, indicates that even our very simple model seems to contain the essential features that describe our films.

### E. Origin of the $T_c$ depression in ultrathin YBCO

In this section we will discuss the various mechanisms that may have an influence on the observed variation of the transition temperature. We have already considered the superconducting proximity effect and concluded that it does not seem to play a major role, since it affects only the superconducting state and not the normal-state conductance. We have also referred to interdiffusion between adjacent layers of different material and suggested that the stepwise increase of  $T_{co}$  and  $G_{\square}$  seen in Figs. 7 and 8 shows that this process also does not have a major effect. In addition the quantitative structural analysis described in Sec. III shows that interdiffusion is small in our specimens. Two remaining mechanisms that we will discuss in detail are the decrease of the electronic mean free path by defects and by the reduction in thickness, and the transfer of charge carriers across the interfaces.

The effect of a decreasing electronic mean free path on the Kosterlitz-Thouless transition has been discussed by Beasley, Mooij, and Orlando.<sup>25</sup> They considered only the “dirty limit,” i.e., the case where the mean free path is short compared to the superconducting coherence length. They derived the relation

$$\frac{T_{KT}}{T_{mf}} = \frac{2.18\hbar}{\epsilon e^2 R_n} \quad (2)$$

initially without the “vortex dielectric constant”  $\epsilon$ , which was later introduced to improve the agreement with experimental results.<sup>26</sup> Since  $T_{mf}$  varies quite slowly compared to  $T_{KT}$  this relation is in qualitative agreement with the linear portion of the graph shown on Fig. 11. A quantitative comparison, however, requires a value for  $\epsilon$  of about 14, a value that seems physically to be quite improbable. It follows that while we cannot rule out some contribution from this mechanism, it does not seem to be the major source of the lowering of  $T_{co}$ .

We now turn to the remaining mechanism, the transfer of charge between adjacent layers, which would change the density of mobile charge carriers in the YBCO and hence also the conductivity.<sup>27</sup> One of the most direct ways to measure the charge density is through the Hall effect, but for the materials that are being considered here the analysis of Hall-effect data is not straightforward. This is primarily because of the strong temperature dependence, which in the absence of a detailed theory makes it unclear how the charge density is to be evaluated. It is plausible, however, that in a given material, and without any other known influences, changes in the

Hall coefficient reflect changes in the density of mobile charge carriers.

Recent measurements on PrBCO/YBCO/PrBCO trilayers indeed show a strong decrease with decreasing YBCO thickness of the “Hall number”  $n = 1/R_{HE}$ , the quantity that for free electrons would be equal to their density.<sup>5</sup> Even though the relation between  $n$  and the actual carrier density is unknown, the data seem to us to be very persuasive in suggesting that the decrease in thickness is accompanied by a decrease in charge density. At 100 K the value of  $n$  for a single-unit-cell layer of YBCO in the trilayer structure is about one third as large as for a thickness of 100 unit-cell layers.

Interestingly, the analysis used in Ref. 5 is based on theoretical considerations that lead the authors to the conclusion that there is almost no change in the actual charge density. They ascribe the change in  $n$  to a change in “skew scattering,” a mechanism that produces asymmetric scattering of conduction electrons from local moments as a result of spin-orbit coupling. This interpretation eliminates all but a minor indication of a change in charge density. The presence of skew scattering has, however, been discussed in detail by Ong,<sup>28</sup> who shows convincingly that it does not make any important contribution in the materials under consideration. It is difficult to escape the conclusion that the change in  $n$  indicated by the Hall-effect data in Ref. 5 indeed reflects a corresponding change in the density of mobile charge carriers.

The link with the change in the transition temperature was demonstrated directly by Xi *et al.*<sup>29</sup> In the experiment described in this reference the charge density in a trilayer structure of SrTiO<sub>3</sub>/YBCO/SrTiO<sub>3</sub> was changed by the application of an electric field. The fractional change in  $T_{co}$  was shown to be equal to the fractional change of the charge density. It seems reasonable that this relation continues to hold beyond the maximum change of about 25% achieved in Ref. 29. We see that if this is the mechanism that accounts for the change in  $T_{co}$  with thickness observed in our measurements, it implies a change in charge density that is quite consistent with the change of  $n$  in the Hall-effect measurements. Support for this view is apparent in the results for the trilayers with the different barrier layers characterized by  $x = 0.50$  and  $0.55$ . These measurements show that the transition temperature increases as  $x$  decreases, in other words, as the barrier layers become less insulating and eventually metallic. Charge transfer to adjacent metallic layers from the YBCO is indeed expected to be less than to the insulating layers of PrBCO.

This effect has also been observed by Norton *et al.*<sup>30</sup> for insulating barrier layers with  $x = 0.7$ , and for metallic barrier layers of Pr<sub>0.5</sub>Ca<sub>0.5</sub>Ba<sub>2</sub>Cu<sub>3</sub>O<sub>7- $\delta$</sub> . These authors, however, rejected an explanation based on charge transfer because the onset temperature seemed not to be affected by the nature of the barrier layers. The onset temperature depends both on the mean-field transition temperature and on the fluctuations. As the superconducting layers become more isolated,  $T_{mf}$  decreases but the fluctuation broadening increases. Since  $T_{mf}$  is, in any case, much less sensitive than  $T_{co}$  to changes in the barrier layers, the experimental results of Norton *et al.*

seem to be entirely in consonance with the results of the present paper.

## F. Surface and bulk conduction

Although Fig. 11 shows a “universal” relationship between  $T_{co}$  and  $G_{\square}$  near the origin, a particular point on the straight line segment corresponds to different thicknesses for the three different barrier-layer materials. In this section we analyze the results further, and introduce a model that casts light on the transition from behavior dominated by the special environment that primarily affects the surface layers to the behavior of the bulk material.

For our point of departure we return to Figs. 8 and 10, which show  $G_{\square}$  as a function of  $d$  for the three series of measurements with different barrier layers. We have already remarked on the striking fact that bulk conduction, characterized on these graphs by a straight line with a slope equal to the bulk conductivity  $\sigma$ , is reached at different values of  $d$  for the different values of  $x$ . The investigation of bulk conduction was not a particular focus of our experiments, and we do not claim that the three straight lines in this region represent the bulk properties with great precision. We have drawn them so as to be consistent with the data, and so as to have the same slope for each of the three series. This slope corresponds to a resistivity of  $60 \mu\Omega$  cm, a value somewhat smaller than that observed for our single thick films. It is quite possible that the much thinner films in the trilayers are indeed more ordered and so lead to lower values of the resistivity.

On the graphs of Figs. 8 and 10 the three straight lines with the slope  $\sigma$  begin at three points  $(G_s, d_s)$ , and can then be described by the equation  $G_{\square} - G_s = \sigma(d - d_s)$ . We may now define the quantity  $G_B \equiv \sigma d$ , as the bulk conductance per square, represented by a straight line through the origin with slope  $d$ , that would be appropriate if bulk conduction started at the origin rather than at  $(G_s, d_s)$ . The actual conductance per square for thicknesses smaller than  $d_s$  is, of course, smaller than the corresponding value of  $G_B$ .

We may now write  $G_B = G_{\square} - G_s + \sigma d_s$ , and use this

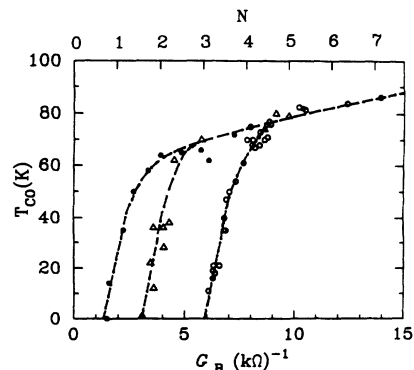


FIG. 13.  $T_{co}$  as a function of  $G_B$ . The symbols are the same as for Fig. 11.



expression to construct the graphs of  $T_{co}$  vs  $G_B$  shown in Fig. 13. Because bulk conductance is reached at different thicknesses for the different series of specimens, this graph separates the three series so as to allow us to follow the change from the “surface regime” below the bend or knee, to the “bulk regime” above. The graph shows strikingly that, as must of course be expected, the bulk regime is independent of the nature of the barrier layer.

Since  $G_B \equiv \sigma d$ , we also show the thickness as measured by the number of unit-cell layers  $N = d/11.8 \text{ \AA}$  along the horizontal axis. We must stress, however, that  $G_B$  is only equal to  $\sigma d$  in the bulk regime, so that the values of  $N$  only have meaning there. The values of  $N$  at the knees determine where the bulk regime is reached for the different barrier layers, but the scale has no meaning in the surface regime.

It may be seen that while the bulk regime is reached at about  $N = 4.5$  for  $x = 1.0$ , it is reached near  $N = 3$  for  $x = 0.55$ , and at about  $N = 2$  for  $x = 0.50$ .

It is also evident that  $T_{co}$  has not reached its bulk value when the bulk regime is first attained. The continued change of the transition temperature may reflect a dependence of the Kosterlitz-Thouless transition on  $d$  in this “clean” regime, but there seems to be no detailed theory that allows us to examine this possibility in detail. It is, of course, also possible that the remaining slow ascent to the bulk value of the transition temperature represents an intrinsic property of the YBCO, i.e. a change that reflects increased coupling between the copper-oxide planes as the specimens progress toward their ultimate three-dimensional properties.

## V. MULTILAYERS

The first measurements on ultrathin films of high- $T_c$  superconductors were done on multilayers because they offer some advantages. The amount of material on which the measurements are performed is larger, the repetitive nature of the specimen gives rise to some inherent averaging, and the superlattice peaks in the x-ray diffraction spectrum can be used to assess and characterize the structure.

Although we have emphasized trilayers because of their greater simplicity we have also measured several series of multilayers, in order to provide a bridge between the two kinds of specimens and to attempt to remove any discrepancies between them.

Figure 14 shows the transition temperatures of YBCO/(Y-Pr)BCO multilayers in which the thickness of the (Y-Pr)BCO barrier layers was kept constant at 400  $\text{\AA}$  while the YBCO thickness,  $d$ , was varied. The upper curves are the onset temperatures, the lower ones are the zero-resistance temperatures,  $T_{co}$ .

The curves show the relatively small but nevertheless significant variation of the onset temperature. The variation of  $T_{co}$ , on the other hand, reflects the differences in the approach to saturation that we have already discussed in connection with the trilayer experiments. The sharp upturn in  $T_{co}$  for  $x = 0.50$ , for example, is in keeping with the observations described earlier and shown on Fig. 13 that for  $d = 24 \text{ \AA}$  this series is already in the bulk

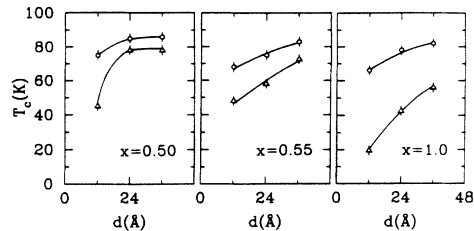


FIG. 14. Transition temperatures for multilayer specimens with 400  $\text{\AA}$  barrier layers and different values of  $x$ . The upper curves are the onset temperatures and the lower curves show  $T_{co}$ .

regime, while for larger  $x$  the surface regime persists to greater thicknesses.

The figure also shows some significant differences from the results for trilayers. In the trilayers the values for  $T_{co}$  for  $d = 24 \text{ \AA}$  with  $x = 1.0$  and  $x = 0.55$  are quite close, at about 39 K. This is not the case for the multilayers of Fig. 14, where  $T_{co}$  for  $x = 1.0$  is close to that in the trilayer, but  $T_{co}$  for  $x = 0.55$  is considerably larger, at about 58 K.

This difference is shown more directly on Fig. 15, which shows  $T_{co}$  as a function of the barrier thickness  $t$ , while the YBCO thickness  $d$  is kept constant at 24  $\text{\AA}$ . Here the trilayer results represent the limiting situation with no coupling between the YBCO regions, corresponding to an infinite barrier thickness. We see, first of all, that the trilayer data fit smoothly on the curves for changing  $t$ , showing that there is no evidence for coupling at length scales larger than a few hundred  $\text{\AA}$ . As  $t$  is reduced, the coupling between YBCO regions increases, consistent with an eventual limit at the bulk value of  $T_{co}$  as  $t$  approaches zero.

It may be seen that for  $x = 0.50$  the variation in  $T_{co}$  is relatively minor, consistent with our previous result that for  $N = 2$  the system is already in the bulk regime for the trilayer. For the insulating barrier, with  $x = 1.0$ , there is a substantial variation in  $T_{co}$  from about 40 K to its bulk value as  $t$  is decreased below about 400  $\text{\AA}$ , where the coupling apparently begins to play a role.

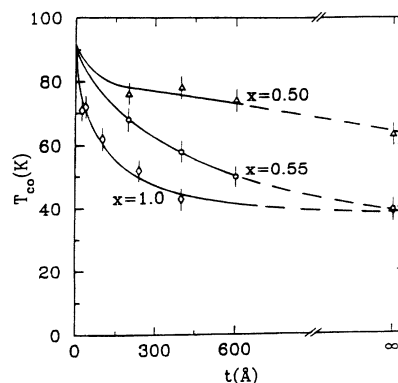


FIG. 15.  $T_{co}$  as a function of the barrier-layer thickness  $t$  for multilayer specimens, all with the same value of  $d$  of 24  $\text{\AA}$ . The points for infinite  $t$  are the trilayer points.

The case of  $x = 0.55$  is particularly interesting, since it shows a change in  $T_{co}$  beginning at even greater values of  $t$ , so that, as mentioned in connection with Fig. 14,  $T_{co}$  is already substantially enhanced when  $t$  is reduced to 400 Å. For this case Fig. 13 shows that the trilayer with  $N=2$  is still in the surface regime, but just barely so. The results shown in Fig. 15 suggest that the decrease in  $t$  in this case not only causes increased coupling, but also brings the YBCO further toward the bulk regime.

The fact that  $T_{co}$  continues to change for values of  $t$  up to at least 400 Å indicates a surprisingly large length scale for this effect. It follows that mechanisms confined to the interface region, such as defects at the interface, cannot explain the changes in transition temperature. Charge transfer can persist over larger distances, although changes up to 400 Å, especially for insulating barriers, are not expected.

If the charge density really changes over such large distances it is possible that for the almost or barely metallic case of  $x = 0.55$  the decrease in  $t$  inhibits charge transfer to some extent and so helps to bring the YBCO into the bulk regime. At the same time the results lead to the strong inference that some other long-range interaction may play an additional role in the coupling between superconducting regions.

## VI. CONCLUSIONS AND REMAINING OPEN QUESTIONS

The results that we describe in this paper lead to the strong implication that transfer of mobile charge carriers across the interfaces is the predominant mechanism responsible for the observed depression of the transition temperature in ultrathin YBCO in multilayer structures. An additional but apparently minor contribution may be expected from the presence of crystalline defects at the interfaces.

Detailed structural investigations have shown that interdiffusion is small at YBCO/PrBCO interfaces and although perhaps not negligible, is unlikely to account for a significant change in the transition temperature. A major contribution from the proximity effect appears also to be ruled out by the strong correlation of the  $T_c$  depression with a corresponding change in the conductance per square, which would presumably not be affected by the proximity effect.

The most important remaining possibility is that there is also an intrinsic size effect, i.e., that coupling along the  $c$  axis from one unit cell to a neighboring unit cell is necessary for the full superconducting properties, including the transition temperature, to be realized. Such an effect may be responsible for the observed change in  $T_{co}$  in the

bulk regime, as seen on Fig. 13.

The change in  $T_{co}$  may also be the result of a shift in the Kosterlitz-Thouless transition in this regime, but the lack of a quantitative theory for this effect in the clean regime prevents a detailed discussion.

We have assumed that the temperature where the resistance goes to zero is determined by the Kosterlitz-Thouless transition. The recent transport measurements on high- $T_c$  superconductors<sup>5,23</sup> strongly support this assumption. We note, however, that early attempts to observe direct evidence for vortex unbinding at  $T_{KT}$  in granular materials were not successful.<sup>31</sup> We are not aware of similar experiments on high- $T_c$  superconductors.

Additional information on the charge transfer process could be obtained by more extensive and specific determinations of the Hall effect. A further direct experiment would be the observation of a change in the carrier density in the barrier layers. For example, a suitably chosen material (with a value of  $x$  just beyond that of the bulk metal-insulator transition) might be shown to become metallic as a result.

Our measurements on multilayer specimens are consistent with those on trilayers, and show a gradual enhancement of the transition temperature as the thickness of the barrier layers is decreased. The length scale of the coupling between superconducting layers is, however, unexpectedly large, so that questions about the mechanism of this coupling remain.

While the results suggest that we now have substantial understanding of the process that leads to the depression of the transition temperature in ultrathin YBCO in trilayers and multilayers with (Y-Pr)BCO, it would clearly be highly desirable to test and extend the conclusions that we have presented here by work on other multilayer systems.

## ACKNOWLEDGMENTS

We are grateful to J. Hasen and I. K. Schuller for the x-ray diffraction measurements and their analysis described in Sec. III B. The refinement program used in the analysis was developed with funds provided by the U.S. Department of Energy and the Belgian Interuniversity Attraction Pole Program. We are also grateful to J. A. Borchers for her collaboration in the x-ray diffraction measurements made at the National Institute of Science and Technology described in the same section. We would like to thank C. H. Nien for his help with the specimen preparation and the measurements. The main part of the research was supported by the National Science Foundation through Grant Nos. DMR 89-17027 and DMR 93-05860, by the Polish Committee for Scientific Research, and by the Rutgers University Research Council.

<sup>1</sup>J.M. Triscone, O. Fischer, O. Brunner, L. Antognazza, A.D. Kent, and M.G. Karkut, Phys. Rev. Lett. **64**, 804 (1990).

<sup>2</sup>Q. Li, X.X. Xi, X.D. Wu, A. Inam, S. Vadlamannati, W.L. McLean, T. Venkatesan, R. Ramesh, D.M. Hwang, J.A. Martinez, and L. Nazar, Phys. Rev. Lett. **64**, 3086 (1990).

<sup>3</sup>D.H. Lowndes, D.P. Norton, and J.D. Budai, Phys. Rev. Lett. **65**, 1160 (1990).

<sup>4</sup>T. Terashima, K. Shimura, Y. Bando, Y. Matsuda, A. Fujiyama, and S. Komiyama, Phys. Rev. Lett. **67**, 1362 (1991).

- <sup>5</sup>Y. Matsuda, S. Komiyama, T. Terashima, K. Shimura, and Y. Bando, *Phys. Rev. Lett.* **69**, 3228 (1992).
- <sup>6</sup>J. Hasen, D. Lederman, and I.K. Schuller, *Phys. Rev. Lett.* **70**, 1731 (1993).
- <sup>7</sup>I.N. Chan, D.C. Vier, O. Nakamura, J. Hasen, J. Guimpel, S. Schultz, and I.K. Schuller, *Phys. Lett. A* **175**, 241 (1993).
- <sup>8</sup>J. Bozovic, J.N. Eckstein, M.E. Klausmeier-Brown, and G. Virshup, *J. Supercond.* **5**, 19 (1992).
- <sup>9</sup>Some of this material has been described in recent brief reports: M.Z. Cieplak, S. Vadlamannati, S. Guha, C.H. Nien, and P. Lindendorf, *Physica C* **209**, 31 (1993); P. Lindendorf, M.Z. Cieplak, S. Guha, S. Vadlamannati, and C.H. Nien, *Physica B* **194-196**, 2157 (1994); S. Guha, M.Z. Cieplak, S. Vadlamannati, C.H. Nien, and P. Lindendorf, *J. Supercond.* **7**, 201 (1994); M.Z. Cieplak, S. Guha, S. Vadlamannati, C.H. Nien, and P. Lindendorf, in *Superconducting Superlattices and Multilayers*, edited by Ivan Bozovic, Proc. SPIE Vol. 2157 (SPIE, Bellingham, WA, 1994), p.222.
- <sup>10</sup>T. Venkatesan, X.D. Wu, B. Dutta, A. Inam, M.S. Hegde, D.M. Hwang, C.C. Chang, L. Nazar, and B. Wilkens, *Appl. Phys. Lett.* **54**, 581 (1989).
- <sup>11</sup>J.J. Neumeier and M.B. Maple, *Physica C* **191**, 158 (1992).
- <sup>12</sup>G. Cao, J. Bolivar, J.W. O'Reilly, J.E. Crow, R.J. Kennedy, and P. Pernambuco-Wise, *Physica B* **186**, 1004 (1993).
- <sup>13</sup>H.L. Kao, J. Kwo, R.M. Fleming, M. Hong, and J.P. Mannearts, *Appl. Phys. Lett.* **59**, 2448 (1991).
- <sup>14</sup>S.J. Pennycook, M.F. Chisholm, D.E. Jesson, D.P. Norton, D.H. Lowndes, R. Feenstra, H.R. Kerchner, and J.O. Thomson, *Phys. Rev. Lett.* **67**, 765 (1991).
- <sup>15</sup>C.L. Jia, H. Soltner, G. Jakob, T. Hahn, H. Adrian, and K. Urban, *Physica C* **210**, 1 (1993).
- <sup>16</sup>Qi Li, T. Venkatesan, and X.X. Xi, *Physica C* **190**, 22 (1991).
- <sup>17</sup>E.E. Fullerton, J. Guimpel, O. Nakamura, and I.K. Schuller, *Phys. Rev. Lett.* **69**, 2859 (1992).
- <sup>18</sup>J.F. Ankner, J.A. Borchers, R.F.C. Farrow, and R.F. Marks, *J. Appl. Phys.* **73**, 6427 (1993).
- <sup>19</sup>I.K. Schuller, *Phys. Rev. Lett.* **44**, 1597 (1980); W. Sev-  
enhans, M. Gijs, Y. Bruynseraede, H. Homma, and I.K. Schuller, *Phys. Rev. B* **34**, 5955 (1986); E. Fullerton, I.K. Schuller, H. Vanderstraeten, and Y. Bruynseraede, *ibid.* **45**, 9292 (1992).
- <sup>20</sup>J.-M. Triscone, P. Fivat, O. Brunner, R. Perez-Pinaya, M. Decroux, and O. Fischer, *J. Alloys Compounds* **195**, 181 (1993).
- <sup>21</sup>K.-Y. Yang, M.S. Dilorio, S. Yoshizumi, M.A. Maung, J. Zhang, P.K. Tsai, and M.B. Maple, *Appl. Phys. Lett.* **61**, 2826 (1992).
- <sup>22</sup>N.-C. Yeh and C.C. Tsuei, *Phys. Rev. B* **39**, 9708 (1989); Q.Y. Ying and H.S. Kwok, *ibid.* **42**, 2242 (1990); D.H. Kim, A.M. Goldman, J.H. Kang, and R.T. Kampwirth, *ibid.* **B40**, 8834 (1989).
- <sup>23</sup>S. Vadlamannati, Q. Li, T. Venkatesan, W.L. McLean, and P. Lindendorf, *Phys. Rev. B* **44**, 7094 (1991).
- <sup>24</sup>L.G. Aslamazov and A.I. Larkin, *Fiz. Tverd. Tela* **10**, 1104 (1968) [*Sov. Phys. Solid State* **10**, 875 (1968)].
- <sup>25</sup>M.R. Beasley, J.E. Mooij, and T.P. Orlando, *Phys. Rev. Lett.* **42**, 1165 (1979).
- <sup>26</sup>J.E. Mooij, in *Percolation, Localization, and Superconductivity*, edited by A.M. Goldman and S.A. Wolf (Plenum, New York, 1984), p. 325; A.F. Hebard and G. Kotliar, *Phys. Rev. B* **39**, 4105 (1989).
- <sup>27</sup>R.F. Wood, *Phys. Rev. Lett.* **66**, 829 (1991); J. Bok, L. Force, and P. Bernstein, *Physica C* **185**, 2067 (1991); I.E. Trofimov, D.H. Leach, A.P. Litvinchuk, K. Kamaras, C. Thomsen, H.-U. Habermeier, and M. Cardona, *ibid.* **209**, 51 (1993).
- <sup>28</sup>N.P. Ong, in *Physical Properties of High Temperature Superconductors II*, edited by D.M. Ginsberg (World Scientific, Singapore, 1990), p. 459.
- <sup>29</sup>X.X. Xi, C. Doughty, A. Walkenhorst, C. Kwon, Q. Li, and T. Venkatesan, *Phys. Rev. Lett.* **68**, 1240 (1992).
- <sup>30</sup>D.P. Norton, D.H. Lowndes, S.J. Pennycook, and J.D. Budai, *Phys. Rev. Lett.* **67**, 1358 (1991).
- <sup>31</sup>P.A. Bancel and K.E. Gray, *Phys. Rev. Lett.* **46**, 148 (1981).